

Evidences of complex formation between DABA-based nucleo- γ -peptides with alternate configuration backbone[‡]

G. N. Roviello,^a D. Musumeci,^{b*} M. Moccia,^a M. Castiglione,^a A. Cesarani,^a E. M. Bucci,^b M. Saviano,^a C. Pedone^a and E. Benedetti^c

In the present work, we report the synthesis and the characterization of *dab* PNA hexamers with diaminobutyric acid backbone of D- or/and L-configuration. In particular, the four nucleo-amino acids we synthesized, D- and L-diaminobutyryl adenines and D- and L-diaminobutyryl thymines, were used in various combinations to assemble the following oligomers: H-G-(t_L-dab)₆-K-NH₂, H-G-(t_D-dab)₆-K-NH₂, H-G-(a_L-dab)₆-K-NH₂, H-G-(t_L-dab-t_D-dab)₃-K-NH₂, H-G-(a_L-dab-a_D-dab)₃-K-NH₂, H-G-(a_L-dab-t_D-dab)₃-K-NH₂. By using CD and UV spectroscopies, we investigated the ability of complementary *dab* PNA strands to bind to each other. We found that binding occurs only between oligomers with backbone of alternate configuration [(t_L-dab-t_D-dab)₃]/[(a_L-dab-a_D-dab)₃] and (a_L-dab-t_D-dab)₃/(a_L-dab-t_D-dab)₃ and implies cooperative hydrogen bonds and base stacking. Furthermore, interesting properties relative to the self-complementary oligomer (a_L-dab-t_D-dab)₃ forming palindromic complexes emerged from preliminary dynamic light-scattering experiments that suggested the formation of multimeric aggregates. These results, together with the high serum stability of the DABA-based oligomers, as shown by HPLC analysis, encourage us to further study *dab* PNAs as new self-recognizing bio-inspired polymers, to develop new nanomaterials in biotechnological and biomedical applications. Copyright © 2008 European Peptide Society and John Wiley & Sons, Ltd.

Keywords: nucleo- γ -peptides; *dab*PNA; alternate-configuration backbone; multimeric aggregates

Introduction

Oligodeoxyribonucleotide (ODN)-like molecules have been widely investigated as therapeutic or diagnostic tools for their ability to bind natural nucleic acids with complementary base sequence [1–4], but recently also for the possibility to develop new self-assembling materials based on hydrogen-bond pairing to be used in bioengineering (nanosensor devices, etc.) and biomedical (hydrogels for drug delivery, etc.) fields [5–7].

*Aeg*PNAs (Figure 1) emerged more than a decade ago as ODN-analogs able to bind, with high affinity and specificity, complementary DNA, RNA, and *aeg*PNA itself, even if several drawbacks, such as low water solubility or poor delivery as well as the absence of optical activity, limit their use in biomedical applications [3,4].

Recently, we synthesized and characterized a modified PNA with DABA backbone that we called *dab*PNA. Moreover, we investigated the binding properties of *dab*PNA-based oligomers toward natural nucleic acids [8,9]. The *dab*PNA nucleo-amino acid is a structural isomer of the *aeg*PNA monomer in which the nucleobase is attached through the usual methylene carbonyl linkage to the α -amino group of the DABA backbone (Figure 1). Compared with Nielsen PNAs, the main features of *dab*PNAs are: (i) a one atom shorter backbone, (ii) a longer distance of the nucleobase from the backbone (one atom more than *aeg*PNAs), (iii) optical activity, and (iv) the absence of binding with natural nucleic acids, as we recently reported [8,9].

Nucleopeptides that are able to hybridize DNA and RNA are interesting for therapeutic and diagnostic purposes, but their usage as biomaterials is also important; for example, extensive molecular networks based on hydrogen-bond pairing of complementary

nucleopeptides could bring to innovative hydrogels for the controlled drug delivery. The use of these kinds of hydrogels would improve the chemical and enzymatic stability of biomaterials and avoid aspecific protein binding of the nucleic acid, if compared with reported systems based on natural oligomers [10–12].

In continuing our research on nucleopeptides for biotechnological applications, we intended to study the potential use of *dab*PNAs in forming molecular networks based on complementary nucleobase recognition. Thus, our investigation was focused on the ability of complementary *dab*PNA strands to bind to each

* Correspondence to: D. Musumeci, Bionucleon Srl, via Montesano 49, Napoli 80131, Italy. E-mail: domymusu@alice.it

a Istituto di Biostrutture e Bioimmagini-CNR, Via Mezzocannone 16, Napoli 80134, Italy

b Bionucleon Srl, via Montesano 49, 80131 Napoli and via Ribes 5, Colletterto Giosca, Torino 10010, Italy

c Università di Napoli 'Federico II', Dip. Scienze Biologiche sez. Biostrutture, via Mezzocannone 16, Napoli 80134, Italy

Abbreviations used: *Aeg*PNA, aminoethylglycylPNA; *Bhoc*, benzhydryloxy carbonyl; *Boc*, tert-butoxycarbonyl; CD, circular dichroism; DABA, diaminobutyric acid; *dab*PNA, diaminobutyrylPNA; DCM, dichloromethane; DIEA, N,N-diisopropylethylamine; DMF, N,N-dimethylformamide; DMSO, dimethylsulfoxide; *Fmoc*, 9-fluorenylmethoxycarbonyl; HATU, O-(7-azabenzotriazol-1-yl)-N,N,N',N'-tetramethyluronium hexafluorophosphate; NMP, 1-methyl-2-pyrrolidone; PyBOP, (1H-benzotriazol-1-yloxy) tripyrrolidinophosphonium hexafluorophosphate; TFA, trifluoroacetic acid; TMP, 2,4,6-trimethylpyridine.

‡ 11th Naples Workshop on Bioactive Peptides.

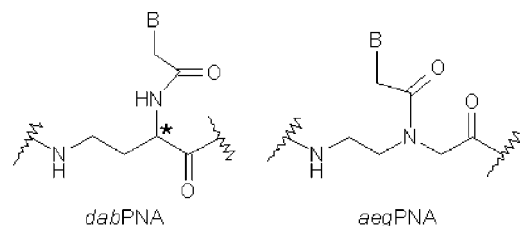


Figure 1. Chemical structures of *dabPNA* and *aegPNA*.

other that is not an obvious property of molecules containing natural DNA nucleobases but artificial backbones.

Materials and Methods

Chemicals

Boc-L-DAB(Fmoc)-OH and Boc-D-DAB(Fmoc)-OH were purchased from Bachem. TFA and Rink-amide resin were from Fluka. Dry CH_3CN , DCM (for synthesis), DIEA and TFA (for HPLC) were from Romil. HATU, PyBOP Fmoc-Gly-OH, and Fmoc-L-Lys(Boc)-OH were purchased from Novabiochem. [N6-(benzhydryloxycarbonyl)-adenine-9-yl] acetic acid was purchased from ASM Research Chemicals GmbH and Co. TMP and deuterated DMSO were from Aldrich. Piperidine was from Biosolve. Anhydroskan DMF and NMP were from LabScan. Solvents for HPLC chromatography and acetic anhydride were from Reidel-de Haën. Perspective Biosystem PNA kit was purchased from PRIMM (Milan, Italy) and included the following reagents: HATU activator, base solution (0.2 M DIEA, 0.3 M lutidine), wash B (anhydrous DMF), capping solution (5% Ac_2O , 6% lutidine), and deblock solution (20% piperidine in DMF). Diethyl ether was from Carlo Erba.

Apparatus

^1H NMR spectra were recorded at 20 °C on Varian Inova 600 MHz spectrophotometer. Chemical shifts (δ) are given in parts per million (ppm) and proton chemical shifts were referenced to residual $\text{CHD}_2\text{SOCD}_3$ ($\delta = 2.49$, quin) signal. Centrifugations were performed on a Z 200 A Hermle centrifuge. Products were analyzed and characterized by LC-MS on an MSQ mass spectrometer (ThermoElectron, Milan, Italy) equipped with an ESI source operating at 3-kV needle voltage and 320 °C, and with a complete Surveyor HPLC system, comprising an MS pump, an autosampler, and a photo diode array (PDA) detector, by using a Phenomenex Jupiter C18 300 Å (5 μm , 4.6 \times 150 mm^2) column. Gradient elution was performed by using increasing amounts of acetonitrile (0.05% TFA) in water (0.05% TFA), monitoring at 260 nm, with a flow rate of 0.8 ml min^{-1} . The monitoring of the reactions in solution and the semi-preparative purifications were performed by RP-HPLC on a Hewlett Packard/Agilent 1100 series, equipped with a diode array detector, by using Phenomenex Juppiter C18 300 Å columns (5 μm , 4.6 \times 150 mm^2 for analyses; 10 μm , 10 \times 250 mm^2 for purifications). Samples were lyophilized in a FD4 Freeze Dryer (Heto Lab Equipment) for 16 h. CD spectra were obtained on a Jasco J-810 spectropolarimeter. UV spectra and UV-melting experiments were recorded on a UV-Vis Jasco model V-550 spectrophotometer equipped with a Peltier ETC-505T temperature controller. UV and CD measurements were performed in Hellma quartz Suprasil cells, with a light path of 1 cm and 2 \times 0.4375 cm (Tandem cell). Dynamic light-scattering (DLS)

experiments were performed on a Viscotek 802 DLS instrument equipped with a 50 mW internal laser operating at a wavelength of 630 nm.

Synthesis of the *dabPNA* Monomers

Commercial Boc-L-DAB(Fmoc)-OH (200 mg, 0.45 mmol) and Boc-D-DAB(Fmoc)-OH (200 mg, 0.45 mmol) were separately reacted with a solution of TFA/DCM/ H_2O 4.5:4.5:1 at 50 °C for 1 h, and subsequently treated as we recently reported [8] (Figure 2). The D- and L-products obtained, dissolved in dry DMF (8 ml) and DIEA (0.6 eq, 41.2 μl , 0.24 mmol) and TMP (0.6 eq, 33.3 μl , 0.24 mmol), were separately reacted with both the thymine-1-acetic acid (2 eq, 149 mg, 0.81 mmol) and the Bhoc-protected adenine-9-acetic acid (2 eq, 149 mg, 0.81 mmol), previously preactivated with HATU (1.9 eq, 293 mg, 0.77 mmol), DIEA (2 eq, 137.5 μl , 0.81 mmol), and TMP (2 eq, 107.0 μl , 0.81 mmol) for 2 min. After 2 h the reaction was quenched by removing the solvent under vacuum, suspending in $\text{H}_2\text{O}/\text{CH}_3\text{CN}$ (7:3) and lyophilizing. The lyophilized crude was resuspended in cold water, sonicated, transferred into a falcon tube, and then centrifuged at 1200 rpm at room temperature. After the supernatant was removed, the white pellet obtained was washed twice with cold water and dried. In this way, products **1** and **2** were obtained as almost pure samples (95% purity), while for **3** and **4** the white pellets were dissolved in $\text{H}_2\text{O}/\text{CH}_3\text{CN}$ 7:3 (v/v) and purified by semi-preparative RP-HPLC using increasing amounts of acetonitrile (from 35 to 75% in 25 min) in water at 25 °C with a flow rate of 4 ml min^{-1} . Pure samples **3** and **4** were obtained as white powders in 51 and 49% yields, respectively. Compound **1**: the LC-ESI-MS and NMR data of **1** were already reported in Ref. 8; compound **2**: the LC-ESI-MS and NMR data of **2** were almost identical to the enantiomer **1**; compound **3**: LC-ESI-MS m/z : 726.36 (found), 726.00 (expected for MH^+); δ_{H} (600 MHz, $\text{DMSO}-d_6$) 8.43 (1H, s, H-8 adenine), 8.22 (1H, s, H-2 adenine), 7.13–7.75 (18H, aromatic CH Fmoc and Bhoc, and 1H Fmoc-NH), 4.47 (2H, s, CH_2 acetyl linker), 4.19–4.50 (4H, m, FmocCH- CH_2 and CH_α), 3.19 (1H, m, part of an AB system centered at 3.22, CH_2NH), 3.25 (1H, m, part of an AB system centered at 3.22, CH_2NH), 2.11 (1H, m, $\text{CH}_2\text{CH}_\alpha$), 1.85 (1H, m, $\text{CH}_2\text{CH}_\alpha$); Compound **4**: the LC-ESI-MS and NMR data were almost identical to the enantiomer **3**.

Solid Phase Syntheses of Oligomers 5–10

Solid phase oligomerizations were carried out in short PP columns (4 ml) equipped with a polytetrafluoroethylene (PTFE) filter, a stopcock and a cap. Solid support functionalization: Rink-amide resin (0.50 mmol NH_2/g , 128 mg) was functionalized with a lysine (Fmoc-Lys(Boc)-OH, 0.5 eq, 14.8 mg, 32 μmol) using PyBOP (0.5 eq, 16.8 mg, 32 μmol) as activating agent and DIEA (1 eq, 12 μl , 64 μmol) as base for 30 min at room temperature. Capping of the unreacted amino groups was performed with Ac_2O (20%)/DIEA (5%) in DMF. Loading of the resin was checked by measuring the absorbance of the released Fmoc group ($\epsilon_{301} = 7800$, quantitative yield) after treatment with a solution of piperidine (30%) in DMF (UV Fmoc test) and resulted reduced to 0.25 mmol g^{-1} with respect to the initial functionalization.

DabPNA monomers were coupled manually to the solid support using the following protocol: a mixture of the monomer (**1–4**) (75 μl of a 0.2 M solution in DMF, 15 μmol , 3 eq), HATU (75 μl of a 0.2 M solution in DMF, 15 μmol , 3 eq), and DMF (100 μl) was introduced into the reactor containing the Rink-amide-Lys- NH_2 resin (0.25 mmol g^{-1} , 20 mg, 5 μmol). Successively, 75 μl (15 μmol ,

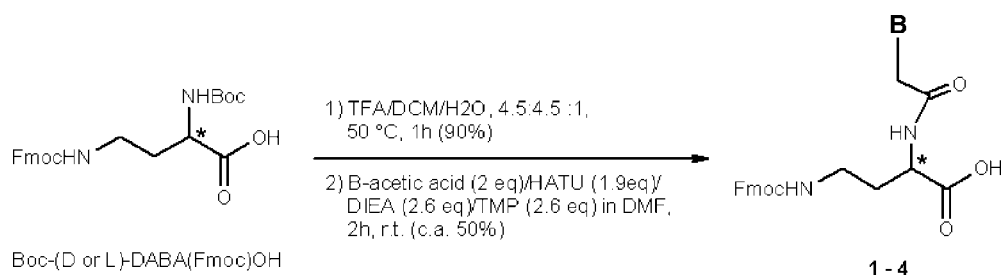


Figure 2. Synthetic procedure to obtain *dab*PNA monomers.

3 eq) of the TMP solution (0.2 M in NMP) was added to the stirred reaction in four portions over 1 h. After the coupling step, unreacted amino groups were capped with PNA capping solution for 5 min. Fmoc removal was accomplished with PNA deblocking solution for 10 min, and was monitored by UV Fmoc test to evaluate the incorporation yields of the monomers. A glycine residue (3 eq) was attached to the N-terminus of all the oligomers by using PyBOP (3 eq)/DIEA (6 eq) as activating system in DMF. After removal and quantification of the final Fmoc group, all oligomers were cleaved from the resin and deprotected under acidic conditions (TFA/*m*-cresol 4 : 1 v/v). After precipitation with cold diethyl ether, centrifugation and lyophilization, crude oligomers, were purified by semi-preparative RP-HPLC at 45 °C using a linear gradient of 5% (for 5 min) to 22% acetonitrile (0.1% TFA) in water (0.1% TFA) over 25 min. Purified oligomers were quantified by UV and characterized by LC-ESI-MS. UV quantification was performed by dissolving oligomers in a known amount of milliQ water and measuring the A_{260} at 85 °C, using as extinction coefficients those of the *aeg*PNA monomers ($\epsilon_{260} = 8600 \text{ cm}^{-1} \text{ M}^{-1}$ for thymine monomer, $\epsilon_{260} = 13700 \text{ cm}^{-1} \text{ M}^{-1}$ for adenine monomer).

H-G-(t_{L-dab})₆-K-NH₂ **5**: HPLC $t_R = 25$ min; UV quantification ($\epsilon_{260} = 51600 \text{ cm}^{-1} \text{ M}^{-1}$) of the purified product gave 110 nmol (2.2% yield); ESI-MS (Figure 3) m/z : 900.07 (found), 900.8 (expected for $[M + 2H]^{2+}$).

H-G-(t_{D-dab})₆-K-NH₂ **6**: HPLC $t_R = 25$ min; UV quantification of the purified product gave 120 nmol (2.4% yield); ESI-MS m/z : 900.17 (found), 900.8 (expected for $[M + 2H]^{2+}$).

H-G-(a_{L-dab})₆-K-NH₂ **7**: HPLC $t_R = 20$ min; UV quantification ($\epsilon_{260} = 82200 \text{ cm}^{-1} \text{ M}^{-1}$) of the purified product gave 204 nmol (4.1% yield); ESI-MS (Figure 3) m/z : 927.9 (found), 927.08 (expected for $[M + 2H]^{2+}$).

H-G-($t_{L-dab-t_{D-dab}}$)₃-K-NH₂ **8**: HPLC $t_R = 23$ min; UV quantification of the purified product gave 95 nmol (1.9% yield); ESI-MS m/z : 900.30 (found), 900.8 (expected for $[M + 2H]^{2+}$).

H-G-($a_{L-dab-a_{D-dab}}$)₃-K-NH₂ **9**: HPLC $t_R = 22$ min; UV quantification of the purified product gave 130 nmol (2.6% yield); ESI-MS m/z : 928.0 (found), 927.08 (expected for $[M + 2H]^{2+}$).

H-G-($a_{L-dab-t_{D-dab}}$)₃-K-NH₂ **10**: HPLC $t_R = 22$ min; UV quantification ($\epsilon_{260} = 66900 \text{ cm}^{-1} \text{ M}^{-1}$) of the purified product gave 140 nmol (2.8% yield); ESI-MS m/z : 915.3 (found), 914.8 (expected for $[M + 2H]^{2+}$).

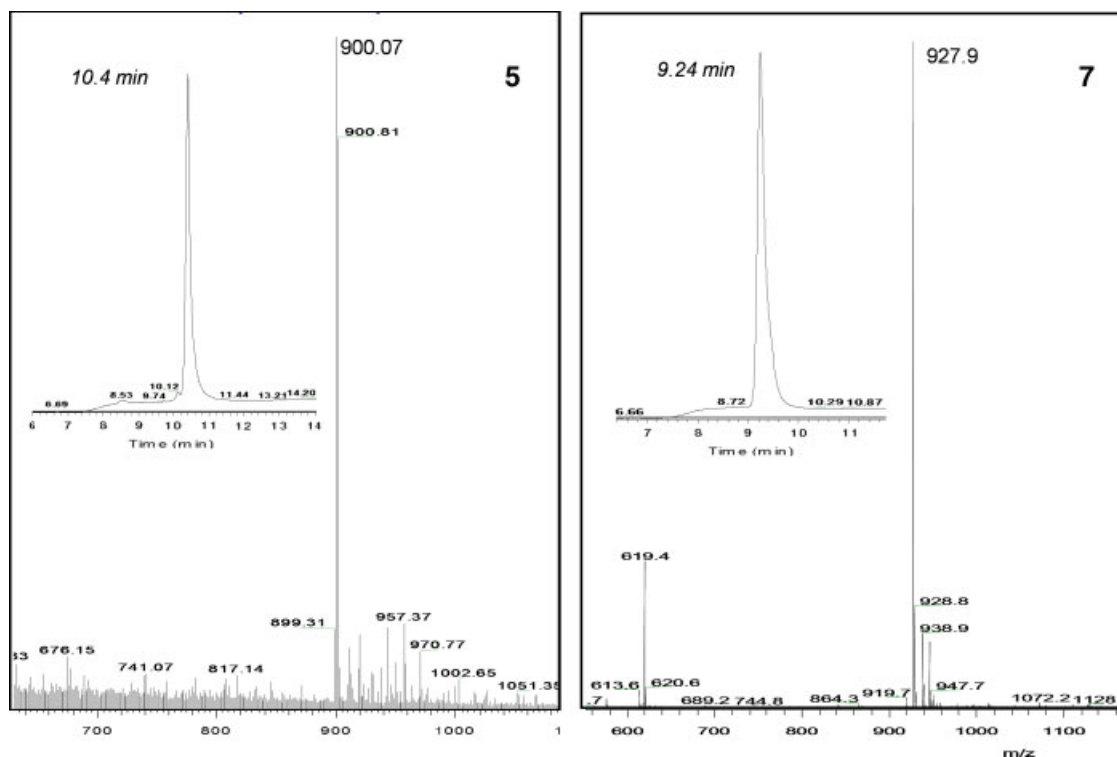


Figure 3. LC-ESI-MS of oligomers **5** and **7**. This figure is available in colour online at www.interscience.wiley.com/journal/jpepsci.

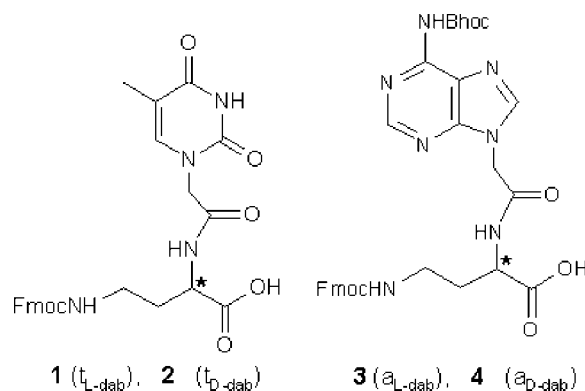


Figure 4. Adenine and thymine *dab*PNA monomers with both D- and L-configurations.

UV and CD Measurements

Annealing of complementary *dab*PNA oligomers was performed by mixing equimolar amounts of the two strands in 10 mM phosphate buffer (pH 7.5). The solution was heated at 85 °C (5 min), allowed to cool slowly to room temperature and then kept at 4 °C for 2 h. Thermal-melting curves were obtained by recording the UV absorbance at 260 nm, while the temperature was increased at a rate of 0.5 °C min⁻¹. T_m values were calculated by the first derivative plot.

CD spectra were recorded from 360 to 200 nm: scan speed 50 nm min⁻¹, data pitch 2 nm, band width 2 nm, response 4 s, ten accumulations. CD-binding experiments were performed with a tandem cell which allows to record the 'sum' spectrum of two separated sample solutions kept each in one of the two reservoirs of the cell, and the 'mix' spectrum obtained after the cell was turned upside down to allow the mixing of the two samples.

Dynamic Light-Scattering Experiments

Hydrodynamic radii of the nucleopeptide complexes were measured via scattered light recorded at 90° angle to incident radiation at a wavelength of 630 nm. From standard autocorrelation functions, measured diffusion coefficients were related to particle hydrodynamic radius via the Stokes–Einstein equation.

Serum Stability Assay

Nucleopeptide **10** (10 µl, 200 µM) was added to 90 µl of 100% fresh human serum (**10** was 10 µM in 90% serum) in a microvial and the mixture was incubated at 37 °C. Aliquots of 10 µl each were taken at times = 0, 1, 2, 24, and 48 h, quenched with 10 µl of 7 M urea solution, kept at 95 °C for 3 min, and then stored at -20 °C until subsequent analysis. The withdrawn samples were analyzed by RP-HPLC on a Phenomenex Juppiter C18 300 Å (5 µm, 4.6 × 250 mm) column using a linear gradient of 8% (for 5 min) to 20% acetonitrile (0.1% TFA) in water (0.1% TFA) over 30 min.

Results and Discussion

In order to realize *dab*PNA hexamers containing adenine and thymine nucleobases inserted on L- and D-DABA backbone, we synthesized the following monomers, suitably protected for the Fmoc solid phase peptide-like synthesis: L-diaminobutyryl thymine (t_{L-dab} , **1**), D-diaminobutyryl thymine (t_{D-dab} , **2**),

L-diaminobutyryl adenine (a_{L-dab} , **3**), and D-diaminobutyryl adenine (a_{D-dab} , **4**, Figure 4).

The synthesis of the four monomers was realized following a procedure that we recently published [8] starting from the commercially available Boc-L-DAB(Fmoc)-OH and Boc-D-DAB(Fmoc)-OH. Briefly, after removal of Boc from the α -amino group of the diaminoacids, they were reacted with both the thyminyl-1-acetic acid and the Bhoc-protected adeninyl-9-acetic acid, as summarized in Figure 2.

Monomers **1** and **2** were purified by precipitation in cold water after removal of DMF. The purification of compounds **3** and **4** was performed by precipitation in cold water followed by RP-HPLC using eluents without TFA to avoid the loss of the acid-labile Bhoc-protecting group. Compounds **1–4** were characterized by NMR and ESI-MS techniques. In particular, ¹H/¹³C-NMR signals and mass spectrum of **1** were in agreement with our previously published data [8], and are the same of the enantiomer **2**. Compound **3** presented, as expected, the same NMR and ESI-MS data of the enantiomer **4**; these data confirmed the identity of the products.

Monomers **1–4** were then used to assemble the following oligomers: H-G-(t_{L-dab})₆-K-NH₂ **5**, H-G-(t_{D-dab})₆-K-NH₂ **6**, H-G-(a_{L-dab})₆-K-NH₂ **7**, H-G-(t_{L-dab} - t_{D-dab})₃-K-NH₂ **8**, H-G-(a_{L-dab} - a_{D-dab})₃-K-NH₂ **9**, and H-G-(a_{L-dab} - t_{D-dab})₃-K-NH₂ **10**. Oligomer synthesis was performed manually on solid phase using Rink-amide support following peptide-like protocols and Fmoc-chemistry. The resin was firstly functionalized with a lysine moiety to improve the solubility of the final products [3]. In order to avoid racemization [8,13,14], coupling steps were performed in DMF/NMP by using HATU, as activator, and by applying a procedure based on the stepwise addition of TMP. Unreacted amino groups on the resin were capped with a mixture of Ac₂O (5%)/lutidine (6%) in DMF, following standard protocols for automated *aeg*PNA synthesis. Deprotection of the γ -amino group from Fmoc (Deblock) was obtained with 20% piperidine in DMF for 10 min. We found experimentally that longer deblocking times were required to obtain better oligomer yields. This represents a further improvement of the procedure we already published for the oligomerization of *dab*PNAs [8]. The efficiency of every coupling step was checked spectrophotometrically by UV Fmoc test. A glycine was added at N-termini of all oligomers to prevent side reactions (*N*-acyl transfer or loss of last residue through cyclization) that occur, as for *aeg*PNAs, when the N-terminal amino group of *dab*PNAs is free in basic or neutral medium [3].

The overall yields of oligomers **5–10**, calculated with respect to the initial functionalization of the Rink-Lys-NH₂ resin on the basis of the Fmoc test on the last residue, ranged from 20 to 25%.

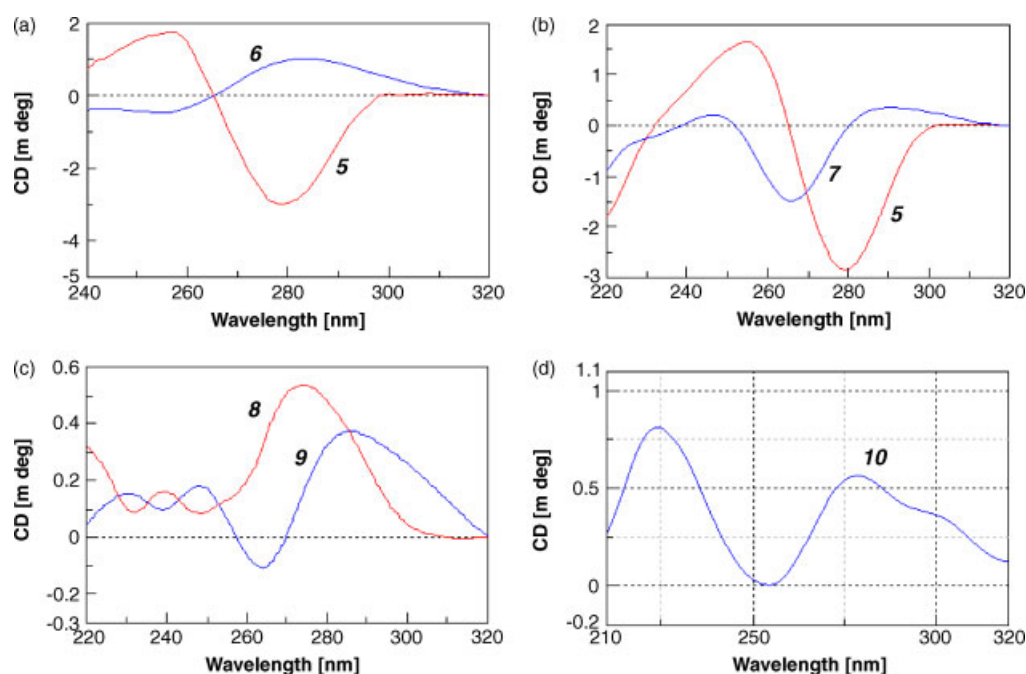


Figure 5. CD spectra in 10 mM phosphate buffer (pH 7.5), 10 °C, 1-cm path length cell, of 4 μ M (a) $(t_{L-dab})_6$ **6**, and $(t_{D-dab})_6$ **5**; (b) $(a_{L-dab})_6$ **7** and $(t_{L-dab})_6$ **5**; (c) $(t_{L-dab-tD-dab})_3$ **8** and $(a_{L-dab-aD-dab})_3$ **9** and (d) $(a_{L-dab-tD-dab})_3$ **10**. This figure is available in colour online at www.interscience.wiley.com/journal/jpepsci.

These yields were lower with respect to those generally reported for the corresponding syntheses of standard *aeg*PNA, because of both the absence of monomers preactivation with HATU, and the stepwise addition of the mild base TMP, which in turn ensure high maintenance of the enantiomeric excess, a fundamental requirement for the subsequent studies on the chiral oligomers.

After deprotection and detachment from the solid support, oligomer **5–10** were purified by RP-HPLC and characterized by LC-ESI-MS (See Experimental Part and Figure 3), which confirmed the identity of the products. All the *dab*PNA hexamers were quantified by UV spectroscopy using the molar extinction coefficients (ϵ_{260}) of the *aeg*PNA monomers, and measuring the A_{260} at 85 °C.

For each oligomer the CD spectrum was recorded in phosphate buffer (pH 7.5). As expected, the CD spectrum of the hexamer **5** (H-G- $(t_{L-dab})_6$ K-NH₂) was similar to that of the analogous dodecamer that we recently published [8], and was approximately the mirror image of **6** (H-G- $(t_{D-dab})_6$ K-NH₂) (Figure 5(a)). The slight deviation of the two spectra from being exactly specular is due to the diastereomeric relationship between **5** and **6** caused by the lysine moiety, which has in both oligomer a L-stereochemistry. Anyway, the observed CD profiles are in agreement with those of other chiral nucleopeptides based on D- and L-ornithine, previously reported in the literature (H- $(t_{L-orn})_{10}$ K-NH₂ and H- $(t_{L-orn})_{10}$ K-NH₂) [13,14].

The homoadenine *dab*PNA **7** with L-chirality presented, analogously to the homothymine strand with the same chirality (**5**), a negative band in the 250–300 nm region with a shift of the minimum from 276 to 266 nm (Figure 5(b)) because of the different chromophores.

CD spectra of the alternate oligomers H-G- $(t_{L-dab-tD-dab})_3$ -K-NH₂ (**8**) and H-G- $(a_{L-dab-aD-dab})_3$ -K-NH₂ (**9**) showed a positive band between 260 and 320 nm with the maxima centered at 274 nm, in the case of **8** and at 284 nm in the case of **9** (Figure 5(c)). The presence of clear CD signals for all oligomers suggested a

structural preorganization of the chiral strands, confirmed by the temperature-dependent CD profiles (data not shown).

In order to investigate if complementary *dab*PNA oligomers bind to each other, CD hybridization studies were performed with a tandem cell, by recording the 'sum' and 'mix' CD spectra of couples of strands. These experiments were performed (i) between *dab*PNA strands of the same chirality [$(t_{L-dab})_6/(a_{L-dab})_6$, **5/7**], (ii) of opposite chirality [$(t_{D-dab})_6/(a_{L-dab})_6$, **6/7**], (iii) between an alternating chirality strand and a homochiral strand [$(t_{L-dab-tD-dab})_3/(a_{L-dab})_6$, **8/7**], and (iv) between two alternating chirality strands [$(t_{L-dab-tD-dab})_3/(a_{L-dab-aD-dab})_3$, **8/9**]. Differences, even if slight, between the 'sum' and 'mix' spectra were observed only in the case of systems **8/7** and **8/9** (Figure 6), suggesting possible hybridizations.

However, UV-melting experiments on the annealed strands revealed a transition phase only in the case of system **8/9** (Figure 7(a), $T_m = 11$ °C), while a drift curve was recorded for the system **7/8**, suggesting a possible transition at a temperature below 5 °C.

Also the self-pairing strand **10** [H-G- $(a_{L-dab-tD-dab})_3$ -K-NH₂], forming palindromic complex with complementary sequences, which showed the CD spectrum reported in Figure 5(d), revealed a transition phase in the UV-melting curve (Figure 7(b)) at 22 °C, confirming the binding between *dab*PNA strands of alternating chirality.

The sigmoidal profile of the UV-melting curves suggested the formation of complexes based on cooperative hydrogen bonds and base stacking. The processes were reversible and the pairing was completed in about 9 °C (18 min at 0.5 °C min⁻¹) for system **8/9** and 18 °C (36 min at 0.5 °C min⁻¹) for system **10**. A further analysis of the melting behavior relative to alternating chirality systems (**8/9** and **10**) revealed very substantial changes in the T_m as a function of the concentration only for the self-assembling system **10**. Thus, for **10** the formation of structures held together by an intricate network of hydrogen bonds based on a stoichiometry of more

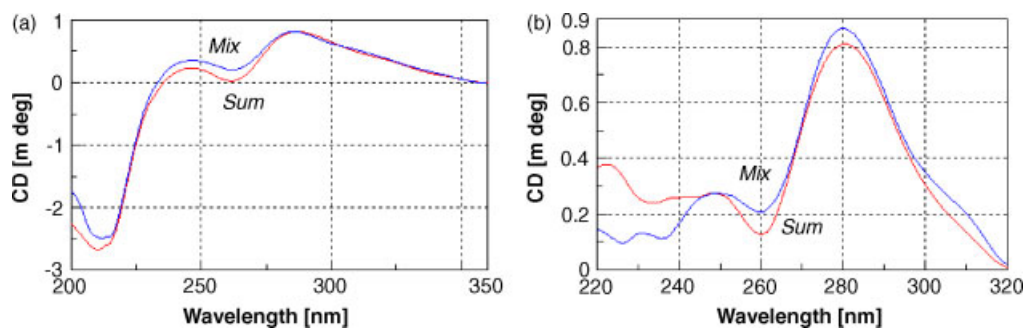


Figure 6. 'Sum' and 'mix' CD spectra of (a) $(a_{L-dab})_6/(t_{L-dab}-t_{D-dab})_3$, **7/8** and (b) $(a_{L-dab}-a_{D-dab})_3/(t_{L-dab}-t_{D-dab})_3$, **9/8**; 4 μM each strand in 10 mM phosphate buffer (pH 7.5). This figure is available in colour online at www.interscience.wiley.com/journal/jpepsci.

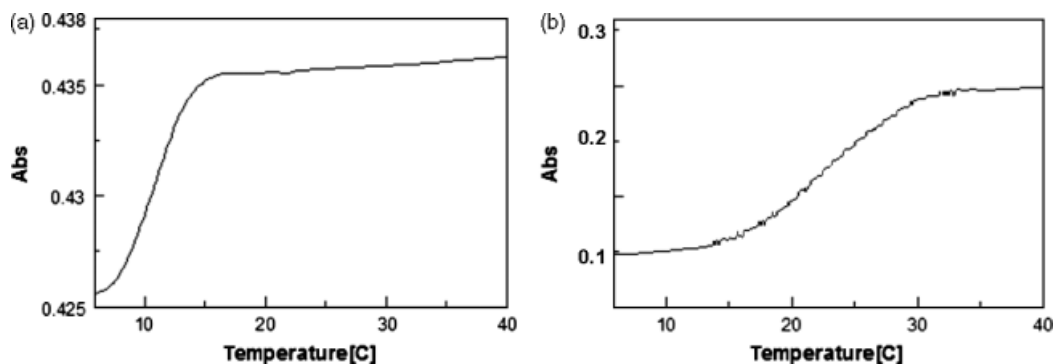


Figure 7. UV-melting experiments of (a) the two-components system $(a_{L-dab}-a_{D-dab})_3/(t_{L-dab}-t_{D-dab})_3$ (**9/8**) and (b) the self-pairing strand $(a_{L-dab}-t_{D-dab})_3$ **10**; (2 μM each strand, in 10 mM phosphate buffer, pH 7.5).

than 1 : 1 should be considered. This hypothesis was supported by preliminary experiments of DLS that revealed for nucleopeptide **10** (100 μM in 10 mM phosphate buffer, pH 7.5), the formation of multimeric aggregates with an molecular weight (MW) ranging between 1.6×10^4 and 4.5×10^5 kDa (with hydrodynamic radii, Rh, comprised between 109 and 634 nm at 16 °C), and between 1.7×10^3 and 4.5×10^4 kDa at 20 °C (Rh reduced to 34–203 nm) (Figure 8).

Further investigations on the viscoelastic properties of system **10** are required to elucidate its bent to form hydrogels; moreover, NMR and X-ray experiments on both **10** and **8/9** complexes are necessary to establish the orientation of the strands (parallel/antiparallel) and whether the Watson–Crick or Hoogsteen pairing is involved. In this frame, large-scale synthesis of oligomers **8**, **9**, and **10** are in progress by our research group. In addition, we are going to synthesize also the C and G *dab*PNA

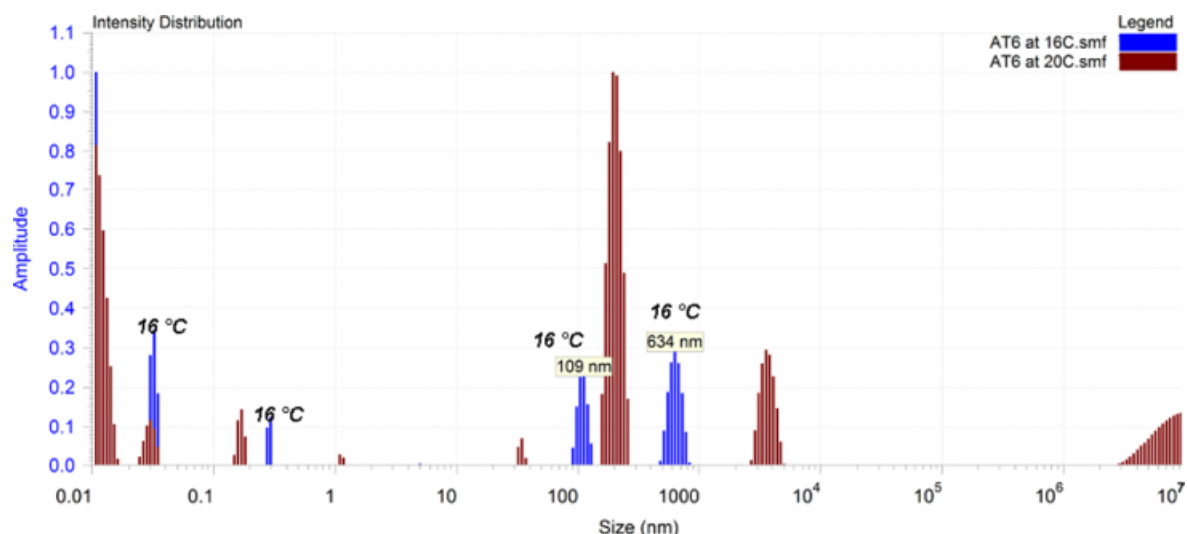


Figure 8. Dynamic light-scattering experiments on the self-complementary *dab*PNA oligomer **10**. This figure is available in colour online at www.interscience.wiley.com/journal/jpepsci.

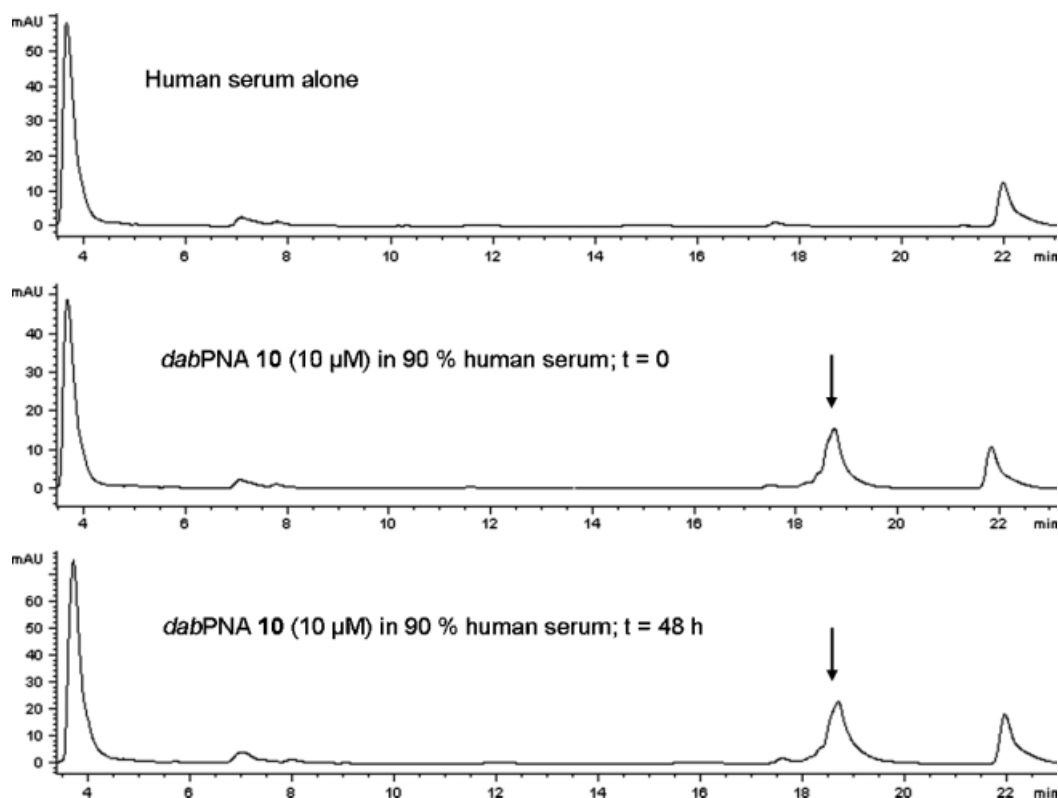


Figure 9. Serum stability assay on *dabPNA 10* performed by HPLC.

monomers to assemble mixed sequence and different length oligomers.

The binding properties of *dabPNAs* could be explained by comparing with the pairing properties of *alanylPNAs* containing an amino acid backbone with alternating configuration [15]. In analogy to *alanylPNAs*, which have a backbone differing from *dabPNA* for two C atoms, we expected for the γ -peptide backbone of *dabPNA* an anti-periplanar orientation of the α -amino group and thus of the nucleobases. When L- and D-configuration is alternate in the backbone, the nucleobases should be orientated in syn-periplanar geometry.

Finally, serum stability assays, performed by HPLC, showed that *dabPNA 10* had a half-life greater than 48 h (Figure 9); even if a good stability to enzymatic degradation is a fundamental characteristic in view of potential bioengineering and biomedical applications of *dabPNAs*, it will be necessary to study the toxicity of these compounds.

Conclusions

In the present work, *dabPNA* oligomers containing adenine and thymine nucleobases and homo- or heterochiral backbones were synthesized and characterized (ESI-MS, CD). In particular, CD characterization of the chiral single strands suggested a structural preorganization, confirmed by the temperature-dependent CD profiles.

We investigated, by using CD and UV spectroscopies, the ability of complementary *dabPNA* strands to bind to each other, which is not an obvious property of molecules with natural DNA nucleobases but artificial backbone. We found that binding occurs only between oligomers with backbone of alternate

configuration. Furthermore, some interesting properties relative to the self-complementary oligomer $(a_{L-dab}-t_{D-dab})_3$ emerged from preliminary DLS experiments that evidenced the formation of multimeric aggregates for this system. These results, together with the high serum stability of the DABA-based oligomers, suggest further studies on *dabPNAs* as new self-recognizing bio-inspired polymers, with the potentiality to develop new nanomaterials or new biotechnological tools in bioengineering and biomedical applications.

Acknowledgements

This work has been funded by the Italian MIUR (FIRB-Contract number RBRN07BMCT). We thank Dr. Giuseppe Perretta for his invaluable technical assistance.

References

1. Kurreck J. Antisense technologies. Improvement through novel chemical modifications. *Eur. J. Biochem.* 2003; **270**: 1628–1644.
2. Braasch DA, Corey DR. Locked nucleic acid (LNA): fine-tuning the recognition of DNA and RNA. *Chem. Biol.* 2001; **8**: 1–7.
3. Uhlmann E, Peyman A, Breipohl G, Will DW. PNA: synthetic polyamide nucleic acids with unusual binding properties. *Angew. Chem., Int. Ed. Engl.* 1998; **37**: 2796–2823.
4. Ray A, Norden B. Peptide nucleic acid (PNA): its medical and biotechnical applications and promise for the future. *FASEB J.* 2000; **14**: 1041–1060.
5. Butler FN, Elibol O, Hines BD, Reddy B Jr, Bashir R, Bergstrom DE. Development of peptide nucleic acid assemblies for application in drug delivery and molecular sensing, NSTI Nanotech 2008, 1–5 June, Boston, MA.
6. Briones C, Martin-Gago JA. Nucleic acids and their analogs as nanomaterials for biosensor development. *Curr. Nanosci.* 2006; **2**: 257–273.

7. Simmel FC. Towards biomedical applications for nucleic acid nanodevices. *Nanomed.* 2007; **2**(6): 817–830.
8. Roviello GN, Moccia M, Sapio R, Valente M, Bucci EM, Castiglione C, Pedone C, Perretta G, Benedetti E, Musumeci D. Synthesis, characterization and hybridization studies of new nucleo- γ -peptides based on diaminobutyric acid. *J. Pept. Sci.* 2006; **12**: 829–835.
9. Roviello GN, Musumeci D, Moccia M, Castiglione M, Sapio R, Valente M, Bucci EM, Perretta G, Pedone C. dabPna: design, synthesis, and dna binding studies. *Nucleosides Nucleotides Nucleic Acids* 2007; **26**: 1307–1310.
10. Luo D, Li Y, Ho Um S, Cu Y. A Dendrimer-like DNA-based vector for DNA delivery: A viral and nonviral hybrid approach. *Methods Mol. Med.* 2006; **127**: 115–126.
11. Lee CK, Shin SR, Lee SH, Jeon JH, So I, Kang TM, Kim SI, Mun JY, Han SS, Spinks GM, Wallace GG, Kim SJ. DNA hydrogel fiber with self-entanglement prepared by using an ionic liquid. *Angew. Chem., Int. Ed. Engl.* 2008; **47**: 2470–2474.
12. Um SH, Lee JB, Park N, Kwon SY, Umbach CC, Luo D. Enzyme-catalysed assembly of DNA hydrogel. *Nat. Mater.* 2006; **5**(10): 797–801.
13. Sforza S, Galaverna G, Dossena A, Corradini R, Marchelli R. Role of chirality and optical purity in nucleic acid recognition by PNA and PNA analogs. *Chirality* 2002; **14**: 591–598.
14. Corradini R, Sforza S, Dossena A, Palla G, Rocchi R, Filira F, Nastri F, Marchelli R. Epimerization of peptide nucleic acids analogs during solid phase synthesis: optimization of the coupling conditions for increasing the optical purity. *J. Chem. Soc., Perkin Trans. 1* 2001; 2690–2696.
15. Diederichsen U. Pairing properties of alanyl peptide nucleic acids containing an amino acid backbone with alternating configuration. *Angew. Chem.* 1996; **108**: 458–461.